P H Y S I C A L   R E V I E W   L E T T E R S

Efficient Generation of Closed Magnetic Flux Surfaces in a Large Spherical Tokamak Using Coaxial Helicity Injection

R. Raman,[1,*] B. A. Nelson,[1] M. G. Bell,[2] T. R. Jarboe,[1] D. Mueller,[2] T. Bigelow,[3] B. LeBlanc,[2] R. Maqueda,[4] J. Menard,[2] M. Ono,[2] and R. Wilson[2]

[1]*University of Washington, Seattle, Washington, USA*
[2]*Princeton Plasma Physics Laboratory, Princeton, New Jersey, USA*
[3]*Oak Ridge National Laboratory, Oak Ridge, Tennessee, USA*
[4]*Nova Photonics, Princeton, New Jersey, USA*
(Received 27 February 2006; published 27 October 2006)

A method of coaxial helicity injection has successfully produced a closed flux current without the use of the central solenoid in the NSTX device, on a size scale closer to a spherical torus reactor, for a proof-of-principle demonstration of this concept. For the first time, a remarkable 60 times current multiplication factor was achieved. Grad-Shafranov plasma equilibrium reconstructions are used to verify the existence of closed flux current. In some discharges the generated current persists for a surprisingly long time ~400 ms.

Until now, almost all tokamaks and spherical torus (ST) plasma confinement devices have relied on a solenoid, through the center of the device, to produce the plasma current (I_p) needed to confine the plasma. Recently, a plasma start-up method called Transient Coaxial Helicity Injection, previously developed on the small HIT-II device [1], has been extended to the much larger NSTX device. The NSTX experiment generated a self-contained ring of plasma carrying 150 kA of closed flux current, for an unambiguous proof-of-principle demonstration of closed flux current generation without the use of the central solenoid (CS). Significant new achievements include (a) a remarkable 60 times current multiplication factor of the injected current, which is an order of magnitude larger than achieved in previous experiments showing a promising favorable size scaling, and (b) fast time scale visible imaging of the entire process that shows discharge evolution, detachment from the injector, and the reconnection of magnetic field lines leading to closed flux formation, with detailed experimental measurements, (c) demonstration of the method in a vacuum vessel volume 30 times larger than HIT-II on a size scale and poloidal field configuration compatible to a compact ST reactor [2]. In some discharges the generated current persists for an unprecedented 400 ms for CHI produced plasmas, which is a surprising and intriguing result. (CHI is a process in which magnetic helicity is injected using coaxial electrodes.) Such an alternate method for plasma start-up is essential for developing a fusion reactor based on the ST concept and could reduce the cost of a future tokamak reactor [3]. Elimination of the CS is essential for the viability of a compact ST reactor. Development of methods for solenoid-free plasma start-up is important for fusion energy development and it is being pursued on other machines [4,5]. CHI is a promising candidate for plasma start-up and for sustained edge current drive [6,7].

The NSTX [major (minor) radius of 0.85 m (0.65 m), elongation ≤ 2.5] vacuum vessel of volume 30 m^3 is fitted with ceramic breaks at the top and bottom so that the central column and the inner divertor plates (cathode) are electrically insulated from the outer divertor plates and the outer vessel components (the anode) as shown in Fig. 1. CHI is implemented by driving current along field lines that connect the inner and outer lower divertor plates (the injector region). A 15 to 45 mF capacitor bank was used at up to 1.8 kV to provide the injector current (I_{inj}). The operational sequence for CHI involves first energizing the toroidal field coils and the CHI injector coils to produce the desired flux conditions in the injector region. The CHI voltage is then applied to the inner and outer divertor plates and a preprogrammed amount of gas and 10 kW of electron cyclotron waves at 18 GHz are injected in a 100 L toroidal cavity below the lower divertor plates. This was an important and essential technical improvement to the NSTX hardware that allowed plasma initiation at conditions where the amount of injected gas is similar to that nominally used as prefill for inductive discharges. This condition ensures that there is adequate energy in the capacitor bank for ionization and heating of the injected gas. The resulting current initially flows along helical magnetic field lines connecting the lower divertor plates. The large ratio of the applied toroidal field to the poloidal field causes the current in the plasma to develop a strong toroidal component, the beginning of the desired toroidal I_p. If I_{inj} exceeds a threshold value, known as the bubble burst condition, the resulting ΔB_{tor}^2 ($J_{pol} \times B_{tor}$) stress across the current layer exceeds the field-line tension of the injector flux (ψ_{inj}) causing the helicity and plasma in the lower divertor region to expand into the main torus chamber. The initial ψ_{inj} magnitude is chosen so that, for the applied voltage, it easily exceeds the bubble burst condition, enabling it to quickly fill the vessel. When I_{inj} is then rapidly decreased,
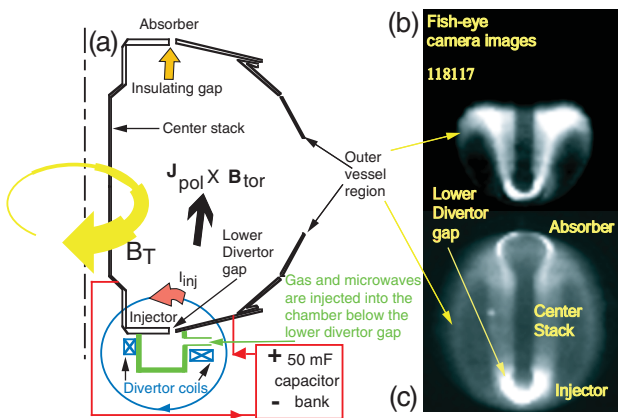
FIG. 1 (color). Shown are (a) the NSTX machine components used for CHI start-up in NSTX and fast camera fish eye images showing (b) discharge evolution from near the injector region and (c) later during the discharge. The bright region at the top of image (b) is the top of the CHI plasma that has extended to approximately the middle of the vessel at a time during the discharge when I_p is below the peak value. As I_p increases to near the peak value, the discharge further elongates vertically to fill the vessel as shown in (c). The bright ring-shaped region at the top of this image is referred to as an absorber arc, a condition when part of I_{inj} bridges the upper divertor gap. Both gas and microwaves are injected in to a 100 L toroidal cavity beneath the lower divertor plates. The gas, which is ionized by the microwaves, emerges from the gap between the lower divertor plates, which eases the requirements for breakdown when the main capacitor bank discharge is initiated.

magnetic reconnection occurs near the injection electrodes, with the toroidal I_p forming closed flux surfaces. A fast visible camera, with a frame rate capability of 64000 frames/s, is used to follow some aspects of the discharge evolution [8].

In Fig. 2, we show traces for I_{inj}, I_p, and fast camera images at two different times during the discharge. Note that the generated toroidal I_p is about 60 times I_{inj}. The CHI capacitor bank discharge is initiated at 5 ms. In these experiments the discharge rapidly grows to fill the vessel within about 2 ms; then starting at about 9 ms the discharge detaches from the injector electrodes. At 11 ms, I_{inj} is zero and about 60 kA of I_p is still present. Note that at 13 ms, the ring-shaped plasma is clearly disconnected from both the injector and the upper divertor plate regions. As time progresses, the large bore plasma that fills the vessel gradually shrinks in size and after about $t = 14$ ms, it evolves into a small diameter plasma ring, as seen in the 15 ms time frame image. For these discharges, circuit calculations show that only about 7 kJ of capacitor bank energy is expended to generate 60 kA of closed flux current. In comparison the CS consumes 450 kJ to reach 60 kA. Electron pressure and temperature profiles from Thomson scattering [9] show that profiles at later times are less hollow than at earlier times. This is consistent with the
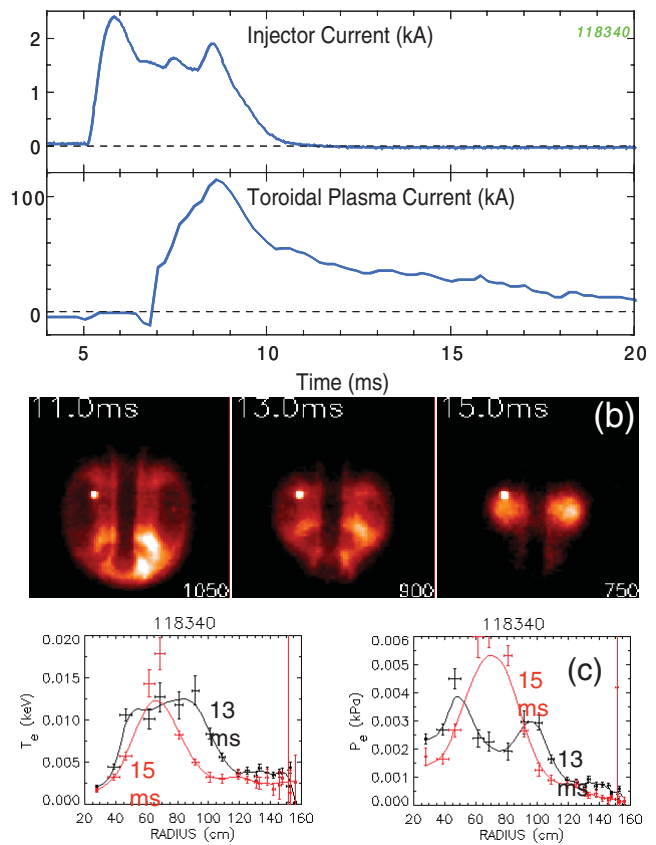

FIG. 2 (color). Shown are (a) I_p and I_{inj} traces, (b) fast camera images, and (c) the electron temperature and electron pressure profiles, at 13 and 15 ms from a CHI discharge in NSTX. The highest measured electron temperatures (not shown here) in transient CHI discharges during the closed flux phase was 30 eV. In this discharge about 2 kA of I_{inj} produces 120 kA of toroidal current resulting in a current multiplication of 60. The best attained current multiplication (not shown here) was 70. During these discharges, the NSTX CS was disconnected from its power supply. The small bright glow is light from a tungsten filament. The images at 11 and 13 ms show an elongated dark region, which is surrounded by a brighter region, like usual tokamak photos. The darker region is probably where most of the toroidal current flows, but because the neutral interaction is strongest in the edge region and because the image brightness is a function of neutral density and electron temperature, the brightness or darkness cannot be directly correlated to the electron current density in these visible camera images. Such images are used as control room diagnostics for discharge development. It is also useful to note that an absorber arc has not been produced in this discharge.

CHI start-up process, since initially CHI drives current at the edge. After reconnection in the injector region, one expects the current profile to flatten, which should result in the profiles becoming less hollow. The evolution of a hollow pressure profile into a peaked pressure profile is shown in Fig. 2(c). The measured electron temperatures of about 30 eV, combined with a plasma inductance of about 0.5–1 μH, should result in an e-folding current decay time

on the order of about 8 ms, which is consistent with the observed current persistence time after I_{inj} has been reduced to zero.

Equilibrium reconstructions from discharge 120874 are shown in Fig. 3. The experimentally measured poloidal magnetic field from 40 sensors and poloidal flux from 44 flux loops are used in the computation of the Grad-Shafranov plasma equilibrium. While equilibrium reconstructions show the presence of closed flux for lower current discharges, such as, for example, the data shown in Fig. 2, equilibrium reconstructions for the recent higher current discharges, such as for shot 120874, are much more robust and result in residuals similar to that in conventional inductive discharges. The χ^2, which is a measure of the residual error, for the fit shown in Fig. 3 is 50. At the time I_{inj} is reduced to zero this discharge has 150 kA of current. After $t = 9$ ms, there is no I_{inj}, and therefore there are no open field-line currents. The only plausible explanation for the decaying current magnitude from 150 to 70 kA at 12 ms
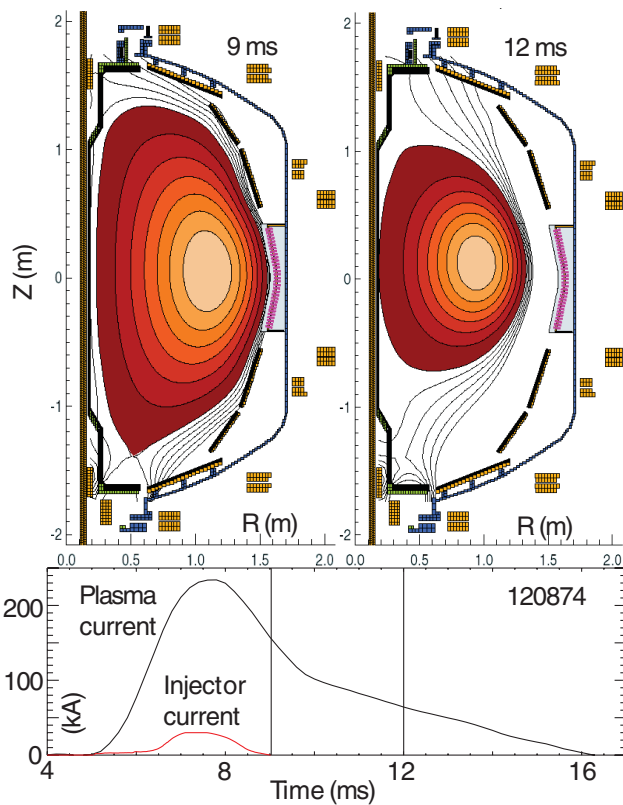

FIG. 3 (color). Equilibrium reconstructions show the shape evolution of the CHI produced plasma in response to decaying current, which is further evidence of decoupling from the injector leaving behind an inductively decaying plasma. In this discharge the increase in I_{inj} around 7.5 ms is due to the presence of an absorber arc. Overdriving the injector by using a larger capacitor bank (45 mF, charged to 1.8 kV) caused a large amount of unused capacitor bank energy to be dissipated as an absorber arc, which probably contributed to an increase in the resistivity of these yet unoptimized discharges.

is that it must result from decaying closed flux equilibrium, which is consistent with the equilibrium reconstructions. The LRDFIT Grad-Shafranov equilibrium code, developed by Menard, which is now in routine use for NSTX discharges, is used for these reconstructions. The code uses a circuit equation model of the plasma, vessel, and passive plate currents to better constrain the equilibrium fits at low I_p.

A result of particular importance for the extrapolation of this method to future machines is that on NSTX the ratio of the generated toroidal current to I_{inj} exceeds 60. This is an order of magnitude larger than the previous experiment on HIT-II, which required about 15 kA of I_{inj} to produce 90 kA of I_p [1]. This very favorable scaling with machine size can be understood from helicity and energy conservation relations [10] that provide the maximum current multiplication factor that could be realized as $I_P = I_{\text{inj}}(\psi_T/\psi_{\text{inj}})$. Here, ψ_T is the toroidal flux inside the vessel [10,11]. For similar values of the toroidal field on axis, NSTX has 10 times more ψ_T than HIT-II. For similar values of ψ_{inj}, current multiplication should be about 10 times better than on HIT-II as observed in this present experiment. Previous work on NSTX has shown that as one reduces ψ_{inj}, the current multiplication increases [12,13]. Second, larger machines require less current to meet the bubble burst condition as there is more volume for the flux to expand into, so they can tolerate a larger flux footprint width, which reduces I_{inj}. The minimum I_{inj} to meet the bubble burst condition is given as $I_{\text{inj}} = 2\psi_{\text{inj}}^2/(\mu_0^2 d^2 I_{\text{TF}})$, where I_{TF} is the current in the toroidal field coil and d is the injector flux footprint width [10]. This scaling suggests that in larger machines, with more than 10 times the ψ_T of NSTX [14], a few kA of I_{inj} should be able to produce MA levels of toroidal current. While the scaling suggests that increasing ψ_T and reducing ψ_{inj} increases the current multiplication and reduces the required I_{inj}, in practice two other optimizations would be required. First, as the ratio ψ_T/ψ_{inj} is increased, the field-line length increases. This increases the injector impedance, which may now require a higher voltage to obtain the same levels of I_{inj}. In Fig. 1 of Ref. [12] the power supply voltage was increased to compensate for the increased injector impedance as ψ_{inj} was reduced to maintain a near constant I_{inj}. Second, the energy transferred by the capacitor bank during the short CHI pulse must exceed the energy required to meet the inductive stored energy in the plasma, $1/2CV^2 > 1/2LI^2$. These requirements would place a limit on the minimum possible I_{inj}. For example, 1 MA ST plasma with an inductance of 0.1 μH would have an inductive stored energy of 100 kJ. At 5 kV operating voltage, a 5 kA I_{inj} pulse for 10 ms transfers 50 C. A 10 mF capacitor bank charged to 5 kV would contain 125 kJ. Eventually, the design limits for voltage hold off and maximum allowable I_{inj} would determine the attainable I_p, with start-up currents of a MA being
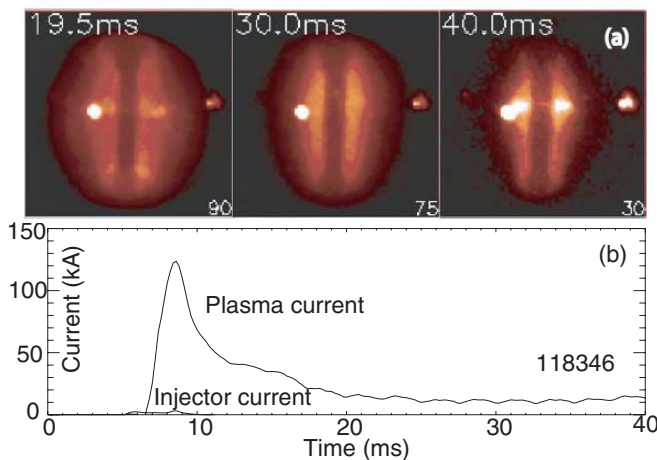
FIG. 4 (color). (a) Shown in the top are fast camera fish eye images during the first 40 ms of a 400 ms discharge. (b) Also shown are I_p and I_{inj}. The small bright image that appears just below and to the left of the plasma ring (in time frame at 40 ms) is light from an electrical filament inside NSTX. The numbers at the bottom of the camera images are maximum scale values for the images.

realizable. Another important aspect of these discharges is that they did not require any special vessel conditioning techniques. The observation on HIT-II was that the best discharges were produced immediately after titanium deposition on the vessel surfaces. After several discharges as the deposited titanium depleted, so did the quality of the CHI discharges. In addition, the present NSTX CHI configuration with divertor plates and relatively few poloidal field coils is more prototypical of the future ST devices. The favorable helicity balance scaling and the prototypical divertor/poloidal field configuration as demonstrated on NSTX bode well to future applications to fusion reactors.

Lastly, the NSTX CHI produced plasma often exhibits the rather curious behavior of very long current persistence as shown in Fig. 4. Initially, the I_p shrinks in size as described above; then starting at about 19 ms, it becomes diffuse and spreads along the center stack. Then, the discharge begins to reduce in elongation, and past 35 ms, it once again becomes a faint small bore plasma that appears to persist for as long as the equilibrium coil currents are not reduced to zero. In the longest duration discharge, a 15 kA discharge remained for nearly 400 ms. A measurement of the electron temperature for these plasmas has not been possible. The electron density is below the threshold for measurement with the Thomson scattering system, which is 1×10^{12} cm^{-3}. A possible explanation is that residual I_p, because of low collisionality and favorable particle drifts, redistributes into a region from which it is not lost because it is trapped in magnetic mirror fields. The pres-

ence of such electrons has been seen in the process of solenoid-free plasma start-up using electron cyclotron waves [15]. In those experiments too, the electrons continue to exist for as long as a suitable vertical field is present and at low collisionality. However, this is the first observation of such long persisting plasmas produced by CHI start-up and without the use of microwave heating.

In summary, the method of transient CHI has been used in NSTX for a proof-of-principle demonstration of closed flux toroidal current generation. In NSTX, 150 kA was produced in a vessel volume on a size scale more comparable to a ST reactor. A remarkable current multiplication factor of up to 60 between the injected current and the achieved toroidal current has been observed. Grad-Shafranov plasma equilibrium reconstructions are used to verify the existence of closed flux current. In some discharges a fraction of the generated current persists for an unprecedented 400 ms, which is an unanticipated and intriguing result. These significant results, which were obtained on a machine designed with mainly conventional components and systems, indicate very favorable scaling toward future devices.

*Electronic address: raman@aa.washington.edu
[1] R. Raman *et al.*, Phys. Rev. Lett. **90**, 075005 (2003).
[2] M. Peng, Plasma Phys. Controlled Fusion **47**, B263 (2005).
[3] F. Najmabadi and The ARIES Team, Fusion Eng. Des. **41**, 365 (1998).
[4] Y. Ono *et al.*, Phys. Rev. Lett. **76**, 3328 (1996).
[5] Y. Takase *et al.*, in *Proceedings of the 20th International Conference on Fusion Energy, Villamoura, Portugal, 2004*, http://www-naweb.iaea.org/napc/physics/fec/fec2004/datasets/EX_P4-34.html.
[6] H. S. McLean *et al.*, Phys. Rev. Lett. **88**, 125004 (2002).
[7] M. Nagata *et al.*, Phys. Plasmas **10**, 2932 (2003).
[8] R. Maqueda (private communication).
[9] B. LeBlanc, Rev. Sci. Instrum. **74**, 1659 (2003).
[10] T. R. Jarboe, Fusion Technol. **15**, 7 (1989).
[11] X. Z. Tang and A. H. Boozer, Phys. Plasmas **12**, 042113 (2005).
[12] R. Raman *et al.*, in *Proceedings of the 29th European Physical Society Conference on Controlled Fusion and Plasma Physics, Montreaux, Switzerland, 2002*, http://epsppd.epfl.ch/Montreux/pdf/P2_103.pdf.
[13] R. Raman *et al.*, Plasma Phys. Controlled Fusion **43**, 305 (2001).
[14] M. Ono *et al.*, Nucl. Fusion **44**, 452 (2004).
[15] M. Uchida *et al.*, IEEJ Trans. FM **125**, 914 (2005).